Marie-Hélène Beauséjour

First *Last*

ASME Paper Title: Numerical Investigation of Spinal Cord Injury After Flexion-Distraction Injuries at the Cervical Spine

Authors: Marie-Hélène Beauséjour, Eric Wagnac, Pierre-Jean Arnoux, Jean-Marc Mac Thiong, Yvan Petit

ASME Journal Title: Journal of Biomechanical Engineering

Volume/Issue 144(1)_______________________ Date of Publication (VOR* Online) September 21, 2021

ASME Digital Collection URL: https://asmedigitalcollection.asme.org/biomechanical/article/144/1/011011/1115612 Investigation-of-Spinal-Cord-Injury

DOI: 10.1115/1.4052003

Numerical Investigation of Spinal Cord Injury After Flexion-Distraction Injuries at the Cervical Spine

Marie-Hélène Beauséjour, first author
Department of Mechanical Engineering, École de technologie supérieure; Research Center, Hôpital du Sacré-Coeur de Montréal; International Laboratory on Spine Imaging and Biomechanics; Laboratoire de Biomécanique Appliquée-Université Gustave-Eiffel; Aix-Marseille Université
1100, rue Notre-Dame Ouest, H3C 1K3, Montreal, Quebec, Canada
marie-helene.beausejour@ens.etsmtl.ca

Eric Wagnac, second author
Department of Mechanical Engineering, École de technologie supérieure; Research Center, Hôpital du Sacré-Coeur de Montréal; International Laboratory on Spine Imaging and Biomechanics
1100, rue Notre-Dame Ouest, H3C 1K3, Montreal, Quebec, Canada
eric.wagnac@etsmtl.ca

Pierre-Jean Arnoux, third author
International Laboratory on Spine Imaging and Biomechanics; Laboratoire de Biomécanique Appliquée-Université Gustave-Eiffel; Aix-Marseille Université
Faculté de Médecine Secteur Nord, Boulevard P. Dramard, 13916, Marseille, France
pierre-jean.arnoux@univ-eiffel.fr

Jean-Marc Mac Thiong, MD, fourth author
Department of Surgery, Medicine Faculty, Université de Montréal; Research Center, Hôpital du Sacré-Coeur de Montréal
5400, boulevard Gouin Ouest, H4J 1C5, Montreal, Quebec, Canada
macthiong@gmail.com

Yvan Petit, fifth author[1]
Department of Mechanical Engineering, École de technologie supérieure; Research Center, Hôpital du Sacré-Coeur de Montréal; International Laboratory on Spine Imaging and Biomechanics
1100, rue Notre-Dame Ouest, H3C 1K3, Montreal, Quebec, Canada
yvan.petit@etsmtl.ca

[1] Corresponding author: Tel : +1 514 396-8691; email : yvan.petit@etsmlt.ca

ABSTRACT

Flexion-distraction injuries frequently causes traumatic cervical spinal cord injury (SCI). Post-traumatic instability can cause aggravation of the secondary SCI during patient's care. However, there is little information on how the pattern of disco-ligamentous injury affects the SCI severity and mechanism. This study objective was to analyze how different flexion-distraction disco-ligamentous injuries affect the SCI mechanisms during post-traumatic flexion and extension. A cervical spine finite element model including the spinal cord was used and different combinations of partial or complete intervertebral disc (IVD) rupture and disruption of various posterior ligaments were modeled at C4-C5, C5-C6 or C6-C7. In flexion, complete IVD rupture combined with posterior ligamentous complex rupture was the most severe injury leading to the most important von Mises stress (47 to 66 kPa), principal strains p1 (0.32 to 0.41 in white matter) and p3 (-0.78 to -0.96 in white matter) in the spinal cord and to the most important spinal cord compression (35 to 48 %). The main post-trauma SCI mechanism was identified as compression of the anterior white matter at the injured level combined with distraction of the posterior spinal cord during flexion. There was also a concentration of the maximum stresses in the gray matter after injury. Finally, in extension, the injuries tested had little impact on the spinal cord. The capsular ligament was the most important structure in protecting the spinal cord. Its status should be carefully examined during patient's management.

INTRODUCTION

Spinal cord injury (SCI) occurs in 34 to 45 % of cervical spine trauma [1–3]. SCI at the cervical level is particularly damageable considering the risk of death and paralysis linked to the position of the segment in the central nervous system. SCI involves two types of mechanism: primary and secondary. Primary SCI is the direct consequence of traumatic vertebral fracture or dislocation leading to spinal canal disruption and excessive deformation or compression of the spinal cord [4]. Secondary SCI is the subsequent aggravation of the neurological impairment and is caused by many different biochemical mechanisms including inflammation [5] and by mechanical instability leading to additional spinal cord disruption during pre-hospital care and early treatment [6]. Following the injury, the spinal cord may remain compressed due to the disrupted spinal canal, translation between vertebrae or damaged structures like a herniated intervertebral disc (IVD) which increase the damage to the spinal cord.

Clinical instability is defined as “the loss of the ability of the spine under physiologic loads to maintain relationships between vertebrae in such a way that there is neither damage nor subsequent irritation to the spinal cord or nerve roots, and, in addition, there is no development of incapacitating deformity or pain due to structural changes” [7]. The integrity of the IVD and ligaments has been recognized as an important component of stability assessment [8,9]. Retrospective clinical studies of hyper-extension have also correlated the integrity of the ligaments and IVD with neurological deficits [10,11].

Flexion-distraction injuries are common at the subaxial cervical spine [12] and especially at C4-C5, C5-C6 and C6-C7 levels [13–15]. They comprise unilateral or bilateral facet subluxations or dislocations, flexion teardrop fractures, chance-type fractures and purely ligamentous injuries [8] and are frequently linked to SCI [16]. Facet dislocation and bilateral facet injury in particular have been identified as significant predictors of SCI in cervical spine trauma [15]. Flexion-distraction injuries present a variety of disco-ligamentous disruption patterns. The injured structures reported for unilateral and bilateral dislocations are the capsular ligaments (CL), the interspinous ligament (ISL), the supraspinous ligament (SSL), the ligamentum flavum (LF), the anterior longitudinal ligament (ALL), the posterior longitudinal ligament (PLL) and the IVD. However, different combinations of disco-ligamentous injuries are observed in different cases. Clinical studies reported that only 40 to 56.5 % of cervical spine dislocation cases had a complete PLL disruption [17,18]. IVD disruption is also variable since different extent of horizontal tear has been observed: complete rupture accompanied with ALL tear or partial rupture [19]. However, little is known about the link between the injured disco-ligamentous structures and the SCI severity.

Many studies have investigated mechanical instability at the cervical spine based on the integrity of disco-ligamentous structures [20–23], but without studying the biomechanical impact on the spinal cord. Liao et al. [24] produced atlanto-occipital dislocation or atlanto-axial instability on cadaver specimens and then analyzed the compression of the dural sac and the cervical spine mobility during the application of a cervical collar. They observed that important motion of the cervical spine and important dural sac compression occurred during cervical collar application. Canal occlusion has also been measured post-trauma in the context of in vitro [25,26] or clinical studies [15,27,28] but with the spine in neutral position only.

Finite element (FE) modeling is a promising solution to study the post-traumatic mechanical damages of the spinal cord since it is possible to test various disco-ligamentous disruption and mechanical loadings without risk of spinal cord degeneration as with in vitro tests. A few FE models of the cervical spine including the spinal cord have been developed. However, they have been exploited under traumatic conditions [29–31] or to study the effect of pathologies or surgical procedures on the spinal cord [32–37]. To our knowledge, no FE study has analyzed the effect of disco-ligamentous injuries on the post-traumatic mechanical integrity of the spinal cord.

The objective of this study was to evaluate how patterns of flexion-distraction disco-ligamentous injuries affect the spinal cord damage in flexion and extension after trauma. A detailed FE model of the cervical spine was used to measure the von Mises stresses and the principal strains in the white and gray matter. The spinal cord compression was also reported.

METHODS

Finite Element Model

For this study, a cervical spine (C2-T1) FE model integrating the spinal cord was used [31,38]. In summary, the geometry of the vertebrae was reconstructed from CT images (0.6 mm contiguous slides) of a healthy 50th percentile male volunteer. In this specific study, the vertebrae were set as rigid bodies. The model had 22.7 degrees of lordosis at C2-C7. The IVD were created between the vertebral endplates and meshed using hexahedral solid elements. They were divided into nucleus pulposus and annulus fibrosus ground substance. IVD mechanical behavior was defined by first-order Mooney-Rivlin hyper-elastic material law representative of non-pathological quasi-static properties [39] (table 1). Collagen fibers were modeled as tension-only springs in the annulus fibrosus ground substance. The springs were organized in concentric lamella with a crosswise pattern of ± 35 degrees. The annulus was divided into three sections (anterior, posterior and lateral) and the collagen fibers force-displacement curves [40] were scaled by a different factor depending on the section [39]. The nucleus properties were calibrated in a previous study [9] to adjust the intradiscal pressure in comparison to in vitro results [41]. The cervical spine ligaments were created between each functional spinal unit (FSU). The geometry and attachment point of the ligaments were based on anatomical data from the literature [42,43]. Each ligament was meshed with 4-nodes shell elements except for the CL (3-nodes shell elements were used) (figure 1). The ligaments behaviors were defined by tabulated non-linear stress-strain curves derived from experimental studies [44,45]. The toe-regions of the curves were calibrated against the intervertebral rotation of each FSU under quasi-static flexion and extension of ± 2 Nm [9]. Facet joints were represented by frictionless contact interfaces.

The spinal cord was meshed using pentahedral solid elements [31]. The geometry of the white and gray matter were based on histological cadaveric spinal cord cross-sections taken from the literature [46]. Tabulated non-linear and strain-rate dependent engineering stress-strain curves were assigned to the white and gray matters [47]. The pia mater was modeled as the external contour of the white matter and the dura mater as the contour of the spinal canal with a 1 mm offset. Both structures were meshed as 4-nodes shell elements. Denticulate ligaments were modeled by 4-nodes shell elements and attached to dura mater lateral sides through coincident nodes (figure 2). The mechanical properties of the dura mater, pia mater and dentate ligaments were represented by linear elastic material properties (table 1). The cerebrospinal fluid was not included into this study. Total number of elements and nodes for this FE model are 506 984 and 154 915 respectively.

Nerve roots were modeled by springs (stiffness of 20 N/mm) attached to the dura matter though a rigid body at the level of the intervertebral foramen (figure 2) and cinematically linked to the superior vertebra at each spinal level. This attachment position was selected since nerve roots are disposed cranially to each spinal level [48] and are attached to the dura mater [49].

Prior to model exploitation, the spinal cord behavior in flexion and extension was validated against values of maximum and minimum principal strain of the spinal cord and relative antero-posterior and superior-inferior displacements of the spinal cord in relation to the vertebrae in healthy subjects at all spinal levels from C3 to C7 and at ± 20 degrees of C2-T1 rotation in flexion-extension [50].

Injury Modeling

For this study, four different types of disco-ligamentous injury patterns were modeled to investigate the relative impact of the structures on the spinal cord protection and represent the diversity of possible flexion-distraction injuries [18,51] (table 2). These injuries were modeled at one spinal level at a time. Three different FSU levels were chosen, C4-C5, C5-C6 and C6-C7 since these levels are the most frequently affected by flexion-distraction injuries [13,14]. This created a total of 12 different injury scenarios. Rupture of a ligament was modeled by removing the corresponding component from the FE model. IVD rupture was represented by a transversal antero-posterior cut into the middle of the disc. A contact interface was added at the rupture between the proximal and distal parts of the disc.

Effects of Injury on the Spinal Cord

After injury modeling, a quasi-static flexion and extension moment (± 2 Nm) was applied to C2 while T1 was kept fixed. This amplitude of moment (± 2 Nm) represents the elastic range of the cervical spine segment [52]. The intact model was submitted to the same loads and used as baseline. This method has been used previously to evaluate intervertebral range of motions after an injury in numerical studies [9,53,54] and was deemed appropriate to evaluate the impact of post-traumatic instability on the spinal cord. The changes in antero-posterior and lateral diameter of the spinal cord during flexion and extension at the level of injury were also analyzed and compared to the SCI threshold of 40 % determined from traumatic cervical spine injury cases [28]. Then, the extreme principal strains p1 and p3 and the von Mises stresses were extracted for five different spinal cord regions: anterior gray matter, gray matter horns, anterior white matter, posterior white matter and lateral white matter. The elements adjacent to the denticulate elements were excluded to avoid stress singularity resulting from the simplified modeling of the denticulate ligaments attachment. The reported data were taken at the maximum applied flexion or extension moment corresponding to 2 Nm or -2 Nm for most cases. For cases where the injuries created a high instability and an unrealistic flexibility, a threshold of evaluation were established at 73 degrees of C2-T1 rotation in flexion which is the maximal sagittal head-torso rotation plus one standard deviation in healthy subjects [55]. C2-T1 rotation could not exceed C0-T1 rotation especially since C1-C2 is very flexible: the chin would touch the torso and no further flexion would be possible.

The strains results were compared to thresholds of neurological deficits determined by experimental studies. Bain et al. [56], in an in vivo animal study, have determined a strain injury threshold of 0.21 for traction loading on the optic nerve. Injury determination was based on measurements of visual evoked potentials. Ouyang et al. [57] tested in compression samples of ex vivo ventral white matter from guinea pig. They measured that the compound action potential diminished starting at 50 % of compression and that this diminution was accelerated after 70 % of compression.

RESULTS

The validation process for the spinal cord showed that the model response fitted generally well with the clinical data [50] (figures 3 and 4) as all the results from the FE model were within one standard deviation of the reference with a few exceptions within two standard deviations. The distribution of p1 strains between the spinal levels respected the trends from the literature, but this was not the case for p3 strains: the strain at the superior spinal levels was more important. The direction of relative displacement was also reversed at C3 for superior-inferior displacement and antero-posterior displacement in flexion.

For extension loading, the impact of the injuries was moderate. In the baseline model at -2 Nm, the maximum principal strain p1 was 0.06 in the gray matter and 0.10 in the white matter and the minimum strain p3 was -0.09 in the gray matter and -0.15 in the white matter. The most extreme principal strain p1 and p3 recorded in the injured models were 0.17 and -0.23 respectively which is under the established thresholds for injury. The spinal cord compression in the antero-posterior and lateral direction in extension was 4 % or less for the uninjured simulation and all the injury scenarios. The maximum von Mises stress was 4.4 kPa in the baseline model at -2 Nm. The difference between the baseline and the injured model was equal or under 2.3 kPa.

For flexion loading, important differences were seen for the different injury cases. The percentage of compression at 2 Nm flexion is presented in figure 5. Percentage of antero-posterior compression in the baseline model was 2 % at C4-C5 and C5-C6 and 1 % at C6-C7. The highest compressions were measured for injury case 4 for every FSU. For injury case 1 and 2, antero-posterior compression stayed under 18 %. The maximum compression measured was 48 % for injury case 4 at C5-C6 in the antero-posterior direction. Generally, the spinal cord compression increased gradually from case 1 to case 4 at all FSU levels. Lateral diameter changes were negligible (under 4 % of difference with baseline for every case).

The extreme principal strains in the spinal cord are presented by axial sections in figures 6 and 7. The maximum p1 strain in the baseline was 0.096 in the gray matter and 0.11 in the white matter. The minimum p3 strain in the baseline was -0.051 in the gray matter and -0.075 in the white matter. For all cases, the injuries had a higher impact on the p3 strain than the p1 strain. In the uninjured model, there is minimal compressive strain and mainly a distractive strain in the posterior spinal cord caused by the flexion of the cervical spine. For the injured cases, this distraction increases up to 0.35. The absolute value of principal strain p1 and p3 increased from case 1 to case 4. The p1 and p3 principal strains were generally uniform in the gray matter, but the posterior gray matter was under more distraction due to the flexion of the spinal cord. In the gray matter, only case 4 injuries had a maximum principal p1 strain over the injury threshold of 0.21 [56]. In the white matter, all case 4 injuries and case 3 at C4-C5 and C6-C7 went over 0.21 of p1 strain. For principal strain p3, only case 4 injuries lead to strains under the – 0.5 threshold for compound action potentials decrease [57] in the white matter and in the anterior gray matter for injury 4 at C5-C6. The threshold of – 0.7 for accelerated compound action potentials was also reached in the anterior white matter in all case 4 injuries and in the lateral white matter for injury case 4 at C5-C6. The anterior and then the lateral white matter were the sections under the most extreme principal strain p3.

Figure 8 shows the distribution of strains (absolute maximum strain) in the spinal cord in flexion for baseline model and injuries cases 1 to 4 at level C4-C5. Flexion of the cervical spine lead to a global distraction in the spinal cord, while the disrupted motion of the injured FSU lead to a band of concentrated compression strain at the injured level. The maximum distraction in the posterior area of the spinal cord went from 0.11 in the baseline model to 0.35 in injury case 4 and is concentrated at the level of injury. Points of compression and distraction are seen at the denticulate ligaments attachments which has also been observed on MRI images of healthy patients [50]. The most extreme principal strains p3 are concentrated in the anterior part of the white matter. This phenomenon was present for every injury scenario, but the amplitude of the compression increases form injury cases 1 to 4, while this area of compression is not present in the baseline model. In the baseline model, the principal strains p3 in the spinal cord were between 0 and -0.075. The same strain pattern was observed for injuries at level C5-C6 and C6-C7.

The maximum von Mises stresses in the spinal cord and their location in the axial cross-section of the spinal cord are presented in table 3. The stress was highest for the case 4 injuries and lead to an increase of 44 to 63 kPa of the maximum von Mises stresses compared to baseline. While the maximum von Mises stress was situated in the posterior white matter in the uninjured model, it moved to the gray matter in all injury cases except for case 1 at C5-C6 where it stayed in the posterior white matter.

The von Mises stress distribution in the spinal cord in flexion for baseline model and injuries cases 1 to 4 at level C4-C5 are shown in figure 9. The stress in the baseline model at 2 Nm flexion is small (under 3 kPa) and concentrated in the posterior spinal cord. In the injured cases, the maximum stress is in the gray matter and mainly in the horns at the injury level.

DISCUSSION

While disco-ligamentous injuries are frequent at the cervical spine [51] and have been linked to instability [8], the relation between the injured structures and the mechanical damage to the spinal cord has not been thoroughly investigated. This study used a C2-T1 FE model including the spinal cord to quantify the effect of various combinations of flexion-distraction disco-ligamentous injuries on the compression of the spinal cord and the strains and stresses in the spinal cord following quasi-static flexion and extension (± 2 Nm). The FE model was validated against clinical data from healthy patients of spinal cord strains and displacements in flexion and extension [50]. The results generally fitted within one standard deviation. Some differences were seen in the relative distribution of p3 strains between spinal levels since the strain at the superior levels was more important. Also, the direction of relative displacements was reversed at C3 in flexion. These differences can be explained by the fact that the upper spinal cord motion is kinematically bound to C2 in the model which could affect the behavior of the spinal cord. Since the injury cases were model at lower spinal levels, these differences seemed acceptable in the context of our study.

In extension, the four disco-ligamentous injury cases studied had little to no impact on the spinal cord. This is partly because the spinous processes acted as a physical barrier and limited the mobility of the injured segment, therefore protecting the spinal cord. Also, the posterior ligaments are mostly loaded in tension as during flexion [58].The intact ALL and, depending on the injury cases, the CL or anterior IVD also retained the stability of the cervical spine in extension. The impact on the spinal cord von Mises stresses (maximum difference of 52 % from baseline) and principal strains (maximum difference of 70 % with baseline) was small compared to flexion loading. Also, the strain injury thresholds determined for SCI were not reached. The spinal cord compression was under 4% which is small compared to the proposed clinical injury threshold of 40 % [28].

In flexion however, the injuries impacted the spinal cord stresses and strains to different degrees depending on the injury case. At all FSU levels, injury case 1, transversal injury of the IVD and posterior ligaments rupture with intact ALL and CL, had little impact on the spinal cord. While this injury case is very unlikely for subluxation or dislocation injuries, it is interesting to analyze the importance of the CL versus the IVD. CL are important in resisting flexion, lateral bending and torsion [21,59] and facets disruption have been linked with neurological deficits [59] which support our finding that, from the disco-ligamentous structures investigated in this paper, the CL was the most important structure for keeping the stability of the segment and protecting the spinal cord. Maeda et al. [11] found that the IVD was associated with segmental instability and neurological impact, but most of their patients were suffering from hyper-extension injury while we studied flexion-type injuries. Richter et al. [23] demonstrated the significant impact of CL rupture on the range of motion in flexion and extension. Pitzen et al. [60] showed that both the CL and IVD are important in stabilizing the cervical spine in flexion and extension. The fact that injury case 4 presented more extreme levels of strains and von Mises stresses than injury case 3, where only 1/3 of the IVD is ruptured posteriorly, shows that the IVD still plays a role in maintaining clinical stability at the cervical spine. All case 4 injuries had principal strains p3 under -0.5 which was determined as a threshold for decrease of compound action potentials in the white matter. This suggests that case 4 injury leads to important aggravation of SCI during cervical spine flexion. The strains and stresses increased from case 1 to case 4 with injury case 4 being the most severe situation. The FSU level of the injury also had an impact on the solicitation of the spinal cord. Since C5-C6 is at the apex of the cervical spine model, injury case 4 caused more damage at this level due to its higher rotation: the highest spinal cord antero-posterior compression and the most extreme strains and stresses. It is also the only case where the threshold of -0.5 of compressive strain was reached in the gray matter. C6-C7 was the only FSU level where injury case 3 reached the extreme C2-T1 rotation of 73 degrees. This can be explained by the superior size of this FSU and its position in the cervical spine. Since T1 is fixed, less motion is necessary for C6-C7 to be at risk of subluxation.

In our study, antero-posterior compression of the spinal cord over 20 % lead to more important levels of stresses and strains than the other cases. Similarly, Kato et al. [61] concluded from a numerical analysis that there may be a critical point in SCI between 20 and 40 % of antero-posterior spinal cord compression as the stress in the cord increased significantly between these two levels. The stresses and strains patterns obtained in this FE study showed that flexion-distraction injury leads to important compressive strains in the anterior spinal cord at the injured FSU level during post-traumatic flexion. The injury mechanism of the spinal cord from flexion-distraction injury has been debated in the literature. The SCI could originate from the excessive traction of the spinal cord during trauma [62] or from shear loading on the spinal cord from the relative translation of the adjacent vertebrae leading to a band of injured tissue at the shear plane [63], while the most extreme form of flexion-distraction injury, dislocation, leads to central lesion impacting principally the gray matter vasculature [64]. From our analysis, the von Mises stress was more important in the gray matter at the level of injury which points toward a central spinal cord lesion. However, the von Mises stress computation is independent of volumetric deformation which should not be neglected in the investigation of potential spinal cord injury. In the baseline model, there were mostly distractive strains in the spinal cord caused by the flexion of the cervical spine. For the injured cases, the distraction in the posterior white matter increased up to 0.35 which is over the 0.21 threshold established for traction loading of optic nerves [56]. This distraction increase is caused by an increase of the flexion range of motion at the injured level and was therefore located at the level of injury. In parallel, the spinal cord was pushed anteriorly onto the vertebra due to high rotation and disturbed antero-posterior motion of the injured level which causes compression of spinal cord and mainly the anterior white matter. This could explain why flexion-distraction leads to important neurological impairment since the blood vessels in the spinal cord are more susceptible to be disrupted by antero-posterior forces [58]. Therefore, at the injured level, the spinal cord is simultaneously susceptible to axons damage at the posterior white matter and disturbance of vascularisation in the gray matter and anterior white matter. However, since this is a post-traumatic study, the mechanism of injury occurring during the trauma cannot be inferred directly from our results.

Limitations of this study linked to model simplification need to be reported. First, the cervical spine was modeled in a neutral erected initial position and no representation of the cervical spine kyphosis linked to hyperflexion sprains [65] or initial subluxation or dislocation was modeled. We believe that these conditions would aggravate the levels of stresses and strains reported but would not change considerably the conclusions regarding the relative impact of the various injuries modeled. The flexion-extension moment of ± 2 Nm used may not be representative of the real-life multidirectional loads that trauma victims experienced. However, this method was necessary to evaluate the effect of a possible post-traumatic spinal instability on the spinal cord. There was no representation of the canal narrowing that can occur from the disruption of disco-ligamentous structures, however this would have probably aggravated the compression of the spinal cord. For example, the material from the IVD could leak in the spinal canal and compress the spinal cord. Muscles were also not represented in this model. While presence of active and passive muscles would have restrained the mobility of the cervical spine, an in vitro study has shown that the instability of the spine is not overestimated if normalized to the intact mobility [66]. There was no representation of the cerebrospinal fluid, however since the load was applied in quasi-static conditions the protective role of the cerebrospinal fluid is negligible. The thresholds used for traction and compression strains were taken from experimental studies of the white matter and not the gray matter, therefore it is difficult to conclude on the effect of the injuries on the gray matter. Finally, the nerve roots were represented only by simple springs. Therefore, it was impossible to determine the impact of the injuries on the stresses and strains of the nerve roots. This could be implemented in a future study.

CONCLUSION

In conclusion, a FE model of the cervical spine was used to quantify how different combinations of disco-ligamentous injuries representative of flexion-distraction trauma impact the principal strains and von Mises stresses in the spinal cord. The analysis showed that these injuries can lead to high strains and stresses in the spinal cord and spinal cord compression of up to 48 % during post-traumatic flexion. On the opposite, extension of the cervical spine had little impact on the spinal cord. The SCI mechanism was identified as an important compression of the anterior spinal cord at the level of injury caused by the relative motion of the vertebrae during flexion following injury with the highest levels of strains in the anterior white matter. Distraction of the posterior white matter is simultaneously present at the injured level and reached the injury threshold for traction. The CL were the structures, in combination with the IVD, that limited the most the solicitation of the spinal cord. These structures should be examined carefully to assess SCI severity.

FUNDING

This research was funded by the Canada research chair in biomechanics of head and spine injuries (grant number 231815) and the Fonds de recherche du Quebec - Nature et technologies (FRQNT) (grant number 271503).

REFERENCES

[1] Hasler, R. M., Exadaktylos, A. K., Bouamra, O., Benneker, L. M., Clancy, M., Sieber, R., Zimmermann, H., and Lecky, F., 2011, “Epidemiology and Predictors of Spinal Injury in Adult Major Trauma Patients: European Cohort Study,” European spine journal, **20**(12), pp. 2174–2180.

[2] Leucht, P., Fischer, K., Muhr, G., and Mueller, E. J., 2009, “Epidemiology of Traumatic Spine Fractures,” Injury, **40**(2), pp. 166–172.

[3] Pickett, G. E., Campos-Benitez, M., Keller, J. L., and Duggal, N., 2006, “Epidemiology of Traumatic Spinal Cord Injury in Canada,” Spine, **31**(7), pp. 799–805.

[4] Jones, C. F., and Clarke, E. C., 2019, “Engineering Approaches to Understanding Mechanisms of Spinal Column Injury Leading to Spinal Cord Injury,” Clinical biomechanics, **64**, pp. 69–81.

[5] Oyinbo, C. A., 2011, “Secondary Injury Mechanisms in Traumatic Spinal Cord Injury: A Nugget of This Multiply Cascade,” Acta Neurobiol Exp (Wars), **71**(2), pp. 281–99.

[6] Engsberg, J. R., Standeven, J. W., Shurtleff, T. L., Eggars, J. L., Shafer, J. S., and Naunheim, R. S., 2013, “Cervical Spine Motion during Extrication,” The Journal of emergency medicine, **44**(1), pp. 122–127.

[7] Panjabi, M., Thibodeau, L., Crisco, J., and White, A., 1988, “What Constitutes Spinal Instability?,” Clinical neurosurgery, **34**, p. 313—339.

[8] Izzo, R., Popolizio, T., Balzano, R. F., Pennelli, A. M., Simeone, A., and Muto, M., 2019, “Imaging of Cervical Spine Traumas,” European journal of radiology.

[9] Beauséjour, M.-H., Petit, Y., Hagen, J., Arnoux, P.-J., Thiong, J.-M. M., and Wagnac, E., 2020, “Contribution of Injured Posterior Ligamentous Complex and Intervertebral Disc on Post-Traumatic Instability at the Cervical Spine,” Computer Methods in Biomechanics and Biomedical Engineering, pp. 1–12.

[10] Song, K.-J., Kim, G.-H., and Lee, K.-B., 2008, “The Efficacy of the Modified Classification System of Soft Tissue Injury in Extension Injury of the Lower Cervical Spine,” Spine, **33**(15), pp. E488–E493.

[11] Maeda, T., Ueta, T., Mori, E., Yugue, I., Kawano, O., Takao, T., Sakai, H., Okada, S., and Shiba, K., 2012, “Soft-Tissue Damage and Segmental Instability in Adult Patients

with Cervical Spinal Cord Injury without Major Bone Injury," Spine, **37**(25), pp. E1560–E1566.

[12] Radcliff, K., and Thomasson, B. G., 2013, "Flexion-Distraction Injuries of the Subaxial Cervical Spine," Elsevier, pp. 45–56.

[13] Allen, J. B., Ferguson, R., Lehmann, T. R., and O'brien, R., 1982, "A Mechanistic Classification of Closed, Indirect Fractures and Dislocations of the Lower Cervical Spine.," Spine, **7**(1), pp. 1–27.

[14] Miller, M. D., Gehweiler, J. A., Martinez, S., Charlton, O. P., and Daffner, R. H., 1978, "Significant New Observations on Cervical Spine Trauma," American Journal of Roentgenology, **130**(4), pp. 659–663.

[15] Quarrington, R. D., Jones, C. F., Tcherveniakov, P., Clark, J. M., Sandler, S. J., Lee, Y. C., Torabiardakani, S., Costi, J. J., and Freeman, B. J., 2018, "Traumatic Subaxial Cervical Facet Subluxation and Dislocation: Epidemiology, Radiographic Analyses, and Risk Factors for Spinal Cord Injury," The Spine Journal, **18**(3), pp. 387–398.

[16] Blauth, M., Mair, G., Schmid, R., Reinhold, M., and Rieger, M., 2007, "Classification of Injuries of the Subaxial Cervical Spine," AO spine manual: clinical applications. Thieme, Stuttgart, pp. 21–38.

[17] Carrino, J. A., Manton, G. L., Morrison, W. B., Vaccaro, A. R., Schweitzer, M. E., and Flanders, A. E., 2006, "Posterior Longitudinal Ligament Status in Cervical Spine Bilateral Facet Dislocations," Skeletal radiology, **35**(7), pp. 510–514.

[18] Vaccaro, A. R., Madigan, L., Schweitzer, M. E., Flanders, A. E., Hilibrand, A. S., and Albert, T. J., 2001, "Magnetic Resonance Imaging Analysis of Soft Tissue Disruption after Flexion-Distraction Injuries of the Subaxial Cervical Spine," Spine, **26**(17), pp. 1866–1872.

[19] Green, J., Harle, T., and Harris, J., 1981, "Anterior Subluxation of the Cervical Spine: Hyperflexion Sprain.," American Journal of Neuroradiology, **2**(3), pp. 243–250.

[20] White, A., Johnson, R., Panjabi, M., and Southwick, W., 1975, "Biomechanical Analysis of Clinical Stability in the Cervical Spine.," Clinical orthopaedics and related research, (109), pp. 85–96.

[21] Goel, V. K., Clark, C. R., McGowan, D., and Goyal, S., 1984, "An In-Vitro Study of the Kinematics of the Normal, Injured and Stabilized Cervical Spine," Journal of biomechanics, **17**(5), pp. 363–376.

[22] Schulte, K., Clark, C. R., and Goel, V. K., 1989, “Kinematics of the Cervical Spine Following Discectomy and Stabilization.,” Spine, **14**(10), pp. 1116–1121.

[23] Richter, M., Wilke, H.-J., Kluger, P., Claes, L., and Puhl, W., 2000, “Load-Displacement Properties of the Normal and Injured Lower Cervical Spine in Vitro,” European Spine Journal, **9**(2), pp. 104–108.

[24] Liao, S., Schneider, N. R., Hüttlin, P., Grützner, P. A., Weilbacher, F., Matschke, S., Popp, E., and Kreinest, M., 2018, “Motion and Dural Sac Compression in the Upper Cervical Spine during the Application of a Cervical Collar in Case of Unstable Craniocervical Junction—A Study in Two New Cadaveric Trauma Models,” PloS one, **13**(4).

[25] Boisclair, D., Mac-Thiong, J.-M., Parent, S., and Petit, Y., 2011, “Effect of Spinal Level and Loading Conditions on the Production of Vertebral Burst Fractures in a Porcine Model,” Journal of biomechanical engineering, **133**(9).

[26] Boisclair, D., Mac-Thiong, J.-M., Parent, S., and Petit, Y., 2013, “Compressive Loading of the Spine May Affect the Spinal Canal Encroachment of Burst Fractures,” Clinical Spine Surgery, **26**(6).

[27] Glassman, D. M., Magnusson, E., Agel, J., Bellabarba, C., and Bransford, R. J., 2019, “The Impact of Stenosis and Translation on Spinal Cord Injuries in Traumatic Cervical Facet Dislocations,” The Spine Journal, **19**(4), pp. 687–694, DOI:10.1016/j.spinee.2018.10.015.

[28] Miyanji, F., Furlan, J. C., Aarabi, B., Arnold, P. M., and Fehlings, M. G., 2007, “Acute Cervical Traumatic Spinal Cord Injury: MR Imaging Findings Correlated with Neurologic Outcome—Prospective Study with 100 Consecutive Patients,” Radiology, **243**(3), pp. 820–827.

[29] Greaves, C. Y., Gadala, M. S., and Oxland, T. R., 2008, “A Three-Dimensional Finite Element Model of the Cervical Spine with Spinal Cord: An Investigation of Three Injury Mechanisms,” Annals of biomedical engineering, **36**(3), p. 396.

[30] Khuyagbaatar, B., Kim, K., Man Park, W., and Hyuk Kim, Y., 2016, “Biomechanical Behaviors in Three Types of Spinal Cord Injury Mechanisms,” Journal of biomechanical engineering, **138**(8).

[31] Bailly, N., Diotalevi, L., Beauséjour, M.-H., Wagnac, É., Mac-Thiong, J.-M., and Petit, Y., 2020, “Numerical Investigation of the Relative Effect of Disc Bulging and Ligamentum Flavum Hypertrophy on the Mechanism of Central Cord Syndrome,” Clinical Biomechanics, **74**, pp. 58–65, DOI:10.1016/j.clinbiomech.2020.02.008.

[32] Taso, M., Fradet, L., Callot, V., and Arnoux, P., 2015, “Anteroposterior Compression of the Spinal Cord Leading to Cervical Myelopathy: A Finite Element Analysis,” Computer methods in biomechanics and biomedical engineering, **18**(sup1), pp. 2070–2071.

[33] Khuyagbaatar, B., Kim, K., Park, W. M., Lee, S., and Kim, Y. H., 2017, “Increased Stress and Strain on the Spinal Cord Due to Ossification of the Posterior Longitudinal Ligament in the Cervical Spine under Flexion after Laminectomy,” Proceedings of the Institution of Mechanical Engineers, Part H: Journal of Engineering in Medicine, **231**(9), pp. 898–906.

[34] Nishida, N., Kanchiku, T., Kato, Y., Imajo, Y., Suzuki, H., Yoshida, Y., Ohgi, J., Chen, X., and Taguchi, T., 2017, “Cervical Ossification of the Posterior Longitudinal Ligament: Factors Affecting the Effect of Posterior Decompression,” The journal of spinal cord medicine, **40**(1), pp. 93–99.

[35] Stoner, K. E., Abode-Iyamah, K. O., Fredericks, D. C., Viljoen, S., Howard, M. A., and Grosland, N. M., 2020, “A Comprehensive Finite Element Model of Surgical Treatment for Cervical Myelopathy,” Clinical Biomechanics, **74**, pp. 79–86, DOI:10.1016/j.clinbiomech.2020.02.009.

[36] Henao, J., Aubin, C.-É., Labelle, H., and Arnoux, P.-J., 2016, “Patient-Specific Finite Element Model of the Spine and Spinal Cord to Assess the Neurological Impact of Scoliosis Correction: Preliminary Application on Two Cases with and without Intraoperative Neurological Complications,” Computer methods in biomechanics and biomedical engineering, **19**(8), pp. 901–910.

[37] Lévy, S., Baucher, G., Roche, P.-H., Evin, M., Callot, V., and Arnoux, P.-J., 2020, “Biomechanical Comparison of Spinal Cord Compression Types Occurring in Degenerative Cervical Myelopathy,” Clinical Biomechanics, p. 105174.

[38] Diotalevi, L., Bailly, N., Wagnac, É., Mac-Thiong, J.-M., Goulet, J., and Petit, Y., 2020, “Dynamics of Spinal Cord Compression with Different Patterns of Thoracolumbar Burst Fractures: Numerical Simulations Using Finite Element Modelling,” Clinical Biomechanics, **72**, pp. 186–194, DOI:10.1016/j.clinbiomech.2019.12.023.

[39] Schmidt, H., Heuer, F., Simon, U., Kettler, A., Rohlmann, A., Claes, L., and Wilke, H.-J., 2006, “Application of a New Calibration Method for a Three-Dimensional Finite Element Model of a Human Lumbar Annulus Fibrosus,” Clinical Biomechanics, **21**(4), pp. 337–344.

[40] Shirazi-Adl, A., Ahmed, A., and Shrivastava, S., 1986, “A Finite Element Study of a Lumbar Motion Segment Subjected to Pure Sagittal Plane Moments,” Journal of biomechanics, **19**(4), pp. 331–350.

[41] Pospiech, J., Stolke, D., Wilke, H. J., and Claes, L. E., 1999, "Intradiscal Pressure Recordings in the Cervical Spine," Neurosurgery, **44**(2), pp. 379–384.

[42] Pintar, F. A., Yoganandan, N., Myers, T., Elhagediab, A., and Sances Jr, A., 1992, "Biomechanical Properties of Human Lumbar Spine Ligaments," Journal of biomechanics, **25**(11), pp. 1351–1356.

[43] Przybylski, G. J., Carlin, G. J., Patel, P. R., and Woo, S. L., 1996, "Human Anterior and Posterior Cervical Longitudinal Ligaments Possess Similar Tensile Properties," Journal of orthopaedic research, **14**(6), pp. 1005–1008.

[44] Mattucci, S. F., Moulton, J. A., Chandrashekar, N., and Cronin, D. S., 2012, "Strain Rate Dependent Properties of Younger Human Cervical Spine Ligaments," Journal of the mechanical behavior of biomedical materials, **10**, pp. 216–226.

[45] Mattucci, S. F., and Cronin, D. S., 2015, "A Method to Characterize Average Cervical Spine Ligament Response Based on Raw Data Sets for Implementation into Injury Biomechanics Models," Journal of the mechanical behavior of biomedical materials, **41**, pp. 251–260.

[46] Kameyama, T., Hashizume, Y., and Sobue, G., 1996, "Morphologic Features of the Normal Human Cadaveric Spinal Cord," Spine, **21**(11), pp. 1285–1290.

[47] Fradet, L., Arnoux, P.-J., Callot, V., and Petit, Y., 2016, "Geometrical Variations in White and Gray Matter Affect the Biomechanics of Spinal Cord Injuries More than the Arachnoid Space," Advances in Mechanical Engineering, **8**(8), p. 1687814016664703.

[48] Cadotte, D., Cadotte, A., Cohen-Adad, J., Fleet, D., Livne, M., Wilson, J., Mikulis, D., Nugaeva, N., and Fehlings, M., 2015, "Characterizing the Location of Spinal and Vertebral Levels in the Human Cervical Spinal Cord," American Journal of Neuroradiology, **36**(4), pp. 803–810.

[49] Reid, J., 1960, "Effects of Flexion-Extension Movements of the Head and Spine upon the Spinal Cord and Nerve Roots," Journal of neurology, neurosurgery, and psychiatry, **23**(3), p. 214.

[50] Stoner, K. E., Abode-Iyamah, K. O., Magnotta, V. A., Howard, M. A., and Grosland, N. M., 2019, "Measurement of in Vivo Spinal Cord Displacement and Strain Fields of Healthy and Myelopathic Cervical Spinal Cord," Journal of Neurosurgery: Spine, **31**(1), pp. 53–59.

[51] Vaccaro, A. R., Hulbert, R. J., Patel, A. A., Fisher, C., Dvorak, M., Lehman Jr, R. A., Anderson, P., Harrop, J., Oner, F. C., and Arnold, P., 2007, "The Subaxial Cervical Spine Injury Classification System: A Novel Approach to Recognize the Importance of

Morphology, Neurology, and Integrity of the Disco-Ligamentous Complex," Spine, **32**(21), pp. 2365–2374.

[52] Wheeldon, J. A., Pintar, F. A., Knowles, S., and Yoganandan, N., 2006, "Experimental Flexion/Extension Data Corridors for Validation of Finite Element Models of the Young, Normal Cervical Spine," Journal of biomechanics, **39**(2), pp. 375–380.

[53] Erbulut, D., Zafarparandeh, I., Lazoglu, I., and Ozer, A., 2014, "Application of an Asymmetric Finite Element Model of the C2-T1 Cervical Spine for Evaluating the Role of Soft Tissues in Stability," Medical engineering & physics, **36**(7), pp. 915–921.

[54] Teo, E., and Ng, H., 2001, "Evaluation of the Role of Ligaments, Facets and Disc Nucleus in Lower Cervical Spine under Compression and Sagittal Moments Using Finite Element Method," Medical engineering & physics, **23**(3), pp. 155–164.

[55] Dvir, Z., and Prushansky, T., 2000, "Reproducibility and Instrument Validity of a New Ultrasonography-Based System for Measuring Cervical Spine Kinematics," Clinical Biomechanics, **15**(9), pp. 658–664.

[56] Bain, A. C., and Meaney, D. F., 2000, "Tissue-Level Thresholds for Axonal Damage in an Experimental Model of Central Nervous System White Matter Injury," J. Biomech. Eng., **122**(6), pp. 615–622.

[57] Ouyang, H., Galle, B., Li, J., Nauman, E., and Shi, R., 2008, "Biomechanics of Spinal Cord Injury: A Multimodal Investigation Using Ex Vivo Guinea Pig Spinal Cord White Matter," Journal of neurotrauma, **25**(1), pp. 19–29.

[58] White, and Panjabi, M., 1990, *Clinical Biomechanics of the Spine*, J. B. Lippincott Company, Philadelphia.

[59] Jaumard, N. V., Welch, W. C., and Winkelstein, B. A., 2011, "Spinal Facet Joint Biomechanics and Mechanotransduction in Normal, Injury and Degenerative Conditions," Journal of biomechanical engineering, **133**(7).

[60] Pitzen, T., Lane, C., Goertzen, D., Dvorak, M., Fisher, C., Barbier, D., Steudel, W.-I., and Oxland, T., 2003, "Anterior Cervical Plate Fixation: Biomechanical Effectiveness as a Function of Posterior Element Injury," Journal of Neurosurgery: Spine, **99**(1), pp. 84–90.

[61] Kato, Y., Kanchiku, T., Imajo, Y., Ichinara, K., Kawano, S., Hamanama, D., Yaji, K., and Taguchi, T., 2009, "Flexion Model Simulating Spinal Cord Injury without Radiographic Abnormality in Patients with Ossification of the Longitudinal Ligament: The Influence of Flexion Speed on the Cervical Spine," The journal of spinal cord medicine, **32**(5), pp. 555–559.

[62] Atesok, K., Tanaka, N., O'Brien, A., Robinson, Y., Pang, D., Deinlein, D., Manoharan, S. R., Pittman, J., and Theiss, S., 2018, "Posttraumatic Spinal Cord Injury without Radiographic Abnormality," Advances in orthopedics, **2018**.

[63] Mattucci, S., Speidel, J., Liu, J., Kwon, B. K., Tetzlaff, W., and Oxland, T. R., 2019, "Basic Biomechanics of Spinal Cord Injury—How Injuries Happen in People and How Animal Models Have Informed Our Understanding," Clinical biomechanics, **64**, pp. 58–68.

[64] Hilton, B. J., Moulson, A. J., and Tetzlaff, W., 2017, "Neuroprotection and Secondary Damage Following Spinal Cord Injury: Concepts and Methods," Neuroscience letters, **652**, pp. 3–10.

[65] Braakman, M., and Braakman, R., 1987, "Hyperflexion Sprain of the Cervical Spine: Follow-up of 45 Cases," Acta orthopaedica Scandinavica, **58**(4), pp. 388–393.

[66] Kettler, A., Hartwig, E., Schultheiss, M., Claes, L., and Wilke, H.-J., 2002, "Mechanically Simulated Muscle Forces Strongly Stabilize Intact and Injured Upper Cervical Spine Specimens," Journal of biomechanics, **35**(3), pp. 339–346.

[67] Toubiana Meyer, R., Sandoz, B., Laville, A., and Laporte, S., 2013, "Parametric Finite Element Modelling of the Human Lower Cervical Spinal Cord," Computer Methods in Biomechanics and Biomedical Engineering, **16**(sup1), pp. 193–194, DOI:10.1080/10255842.2013.815893.

[68] Ozama, H., Matsumoto, T., Ohashi, T., Ohashi, T., Sato, M., and Kokubun, S., 2004, "Mechanical Properties and Function of the Spinal Pia Matter," J Neurosurg Spine, **1**, pp. 122–127.

[69] Polak-Kraśna, K., Robak-Nawrocka, S., Szotek, S., Czyż, M., Gheek, D., and Pezowicz, C., 2019, "The Denticulate Ligament–Tensile Characterisation and Finite Element Micro-Scale Model of the Structure Stabilising Spinal Cord," Journal of the mechanical behavior of biomedical materials, **91**, pp. 10–17.

Figure Captions List

Fig. 1	Cervical spine model. Left: lateral view of the entire finite element model with boundary conditions. Right: sagittal cross-section of a functional spinal unit
Fig. 2	Central Nervous System. Left: axial cross-section. Right: lateral view of the left C6-C7 nerve root
Fig. 3	Maximum and minimum principal strains. Error bars represent one standard deviation
Fig. 4	Relative antero-posterior displacements and superior-inferior displacements. Error bars represent one standard deviation
Fig. 5	Percentage of spinal cord compression at the injured functional spinal unit at 2 Nm flexion. Asterisk (*) represents the C2-T1 73 degrees threshold
Fig. 6	Maximum principal strains p1 in spinal cord by sections at 2 Nm flexion. Asterisk (*) represents the C2-T1 73 degrees threshold
Fig. 7	Minimum principal strains p3 in spinal cord by sections at 2 Nm flexion. Asterisk (*) represents the C2-T1 73 degrees threshold
Fig. 8	Absolute maximal strain pattern for baseline model and injury models at level C4-C5
Fig. 9	von Mises stress pattern for baseline model and injury models at level C4-C5

Table Caption List

Table 1	Material properties of the finite element model structures
Table 2	Type of disco-ligamentous injury patterns
Table 3	Maximum von Mises stress in the spinal cord. Asterisk (*) represents the C2-T1 73 degrees threshold

Table 1: Material properties of the finite element model structures

Structure	Material Law	Material parameters	Reference
Dura mater	Linear elastic	E = 5 MPa $\upsilon = 0.45$	[67]
Pia mater	Linear elastic	E = 2.3 MPa $\upsilon = 0.45$	[68]
Denticulate Ligaments	Linear elastic	E = 3.8 MPa $\upsilon = 0.4$	[69]
White Matter	Stress-strain tabulated	$\upsilon = 0.38$	[47]
Gray Matter	Stress-strain tabulated	$\upsilon = 0.38$	[47]
Annulus fibrosus	First-order Mooney-Rivlin hyper-elastic material law	$\upsilon = 0.495$ $C_{10} = 0.18$ $C_{01} = 0.045$	[39]
Nucleus	First-order Mooney-Rivlin hyper-elastic material law	$\upsilon = 0.45$ $C_{10} = 0.24$ $C_{01} = 0.18$	[9, 39]
Collagen fibers	Force-displacement tabulated		[9, 39, 40]
Spinal ligaments	Stress-strain tabulated specific to each ligament type	$\upsilon = 0.45$	[9, 44, 45]

Table 2: Type of disco-ligamentous injury patterns

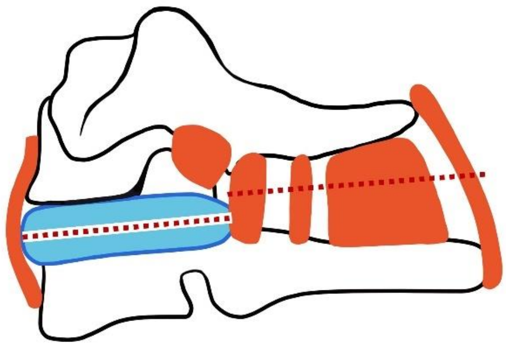	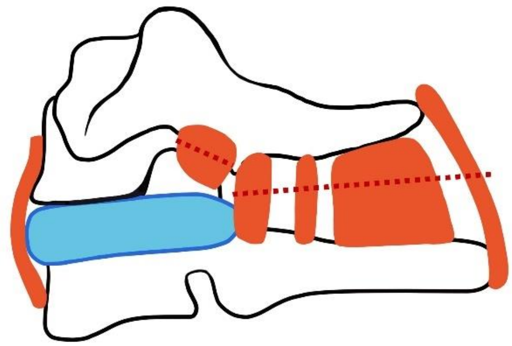
Case 1 - Rupture of the interspinous ligament, ligamentum flavum, supraspinous ligament and posterior longitudinal ligament accompanied with a transversal rupture of the intervertebral disc	Case 2 - Rupture of the interspinous ligament, ligamentum flavum, supraspinous ligament and posterior longitudinal ligament accompanied with rupture of the capsular ligament
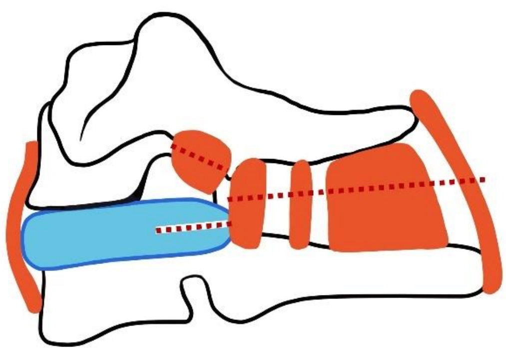	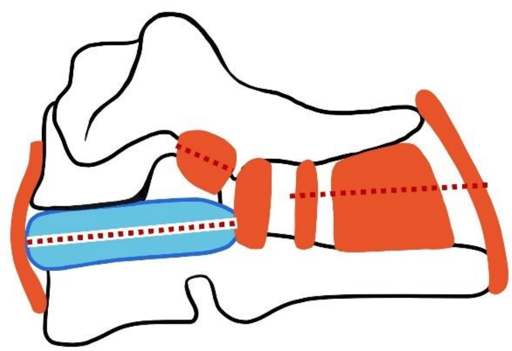
Case 3 - Rupture of the interspinous ligament, ligamentum flavum and supraspinous ligament accompanied with rupture of the capsular ligament and a partial transversal rupture of the intervertebral disc (1/3 of the disc length)	Case 4 - Rupture of the interspinous ligament, ligamentum flavum and supraspinous ligament with rupture of the capsular ligament and transversal rupture of the intervertebral disc. The posterior longitudinal ligament is kept intact.

Table 3: Maximum von Mises stress in the spinal cord. Asterisk (*) represents the C2-T1 73 degrees threshold

Model		Maximum von Mises stress (kPa)	Section
	Baseline	2.8	Posterior white matter
Injury Level	**Injury case**		
C4-C5	Case 1	6.2	Anterior gray matter
	Case 2	25	Gray matter horns
	Case 3	29	Gray matter horns
	Case 4	58*	Gray matter horns
C5-C6	Case 1	2.9	Posterior white matter
	Case 2	4.5	Gray matter horns
	Case 3	9	Gray matter horns
	Case 4	66*	Anterior white matter
C6-C7	Case 1	4.3	Gray matter horns
	Case 2	7.7	Gray matter horns
	Case 3	32*	Gray matter horns
	Case 4	47*	Anterior gray matter

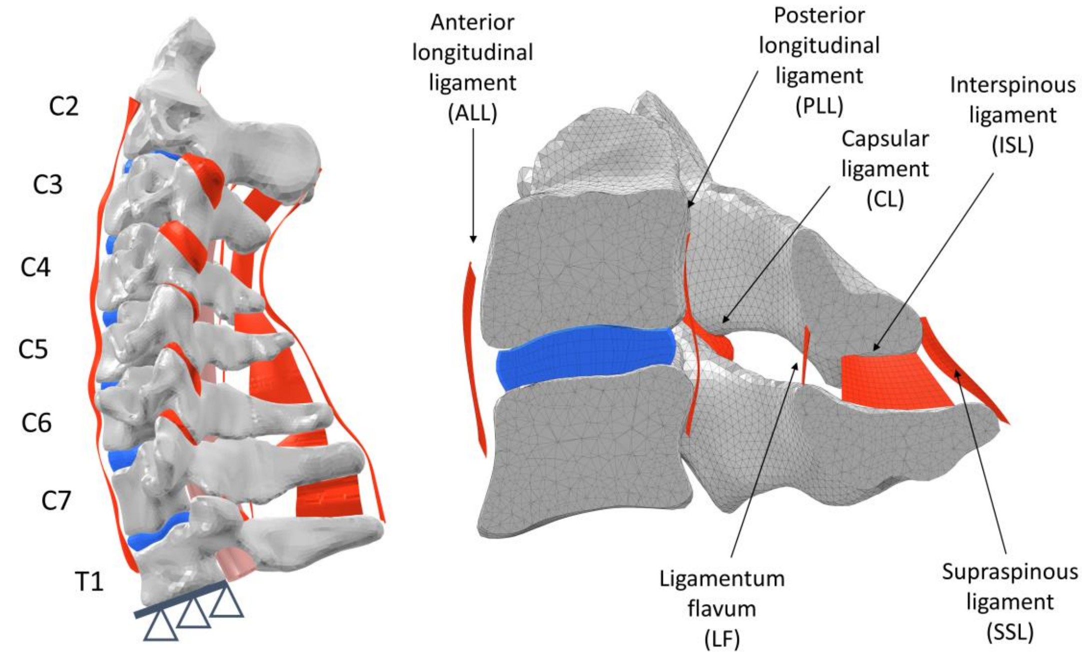

Figure 1: Cervical spine model. Left: lateral view of the entire finite element model with boundary conditions. Right: sagittal cross-section of a functional spinal unit

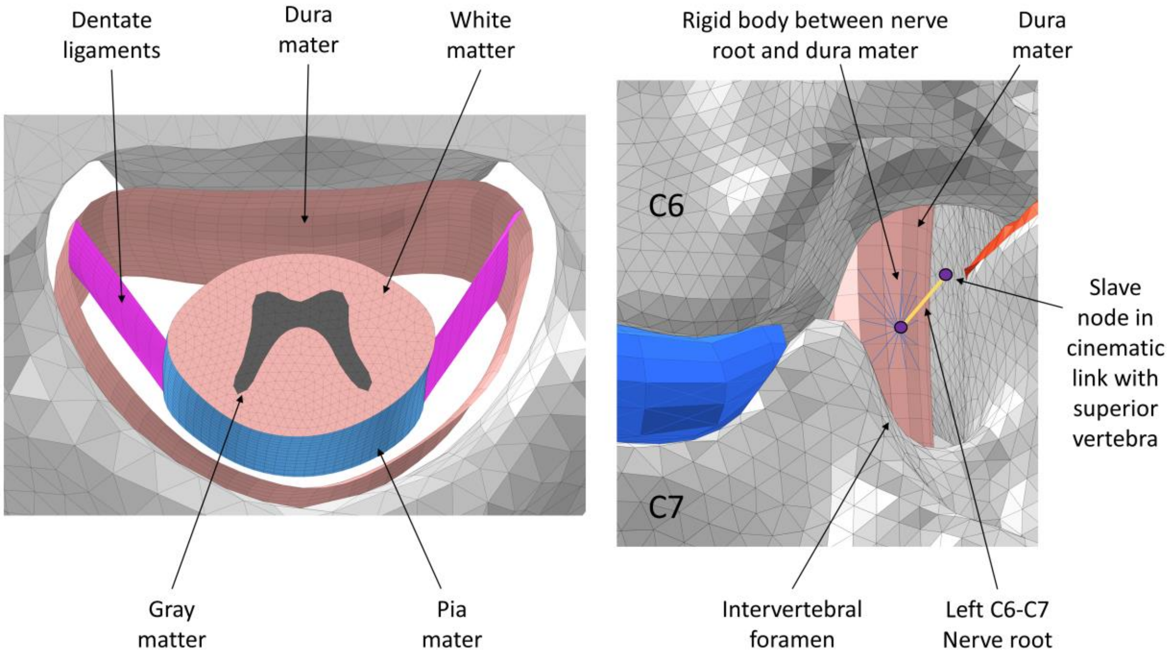

Figure 2: Central Nervous System. Left: axial cross-section. Right: lateral view of the left C6-C7 nerve root

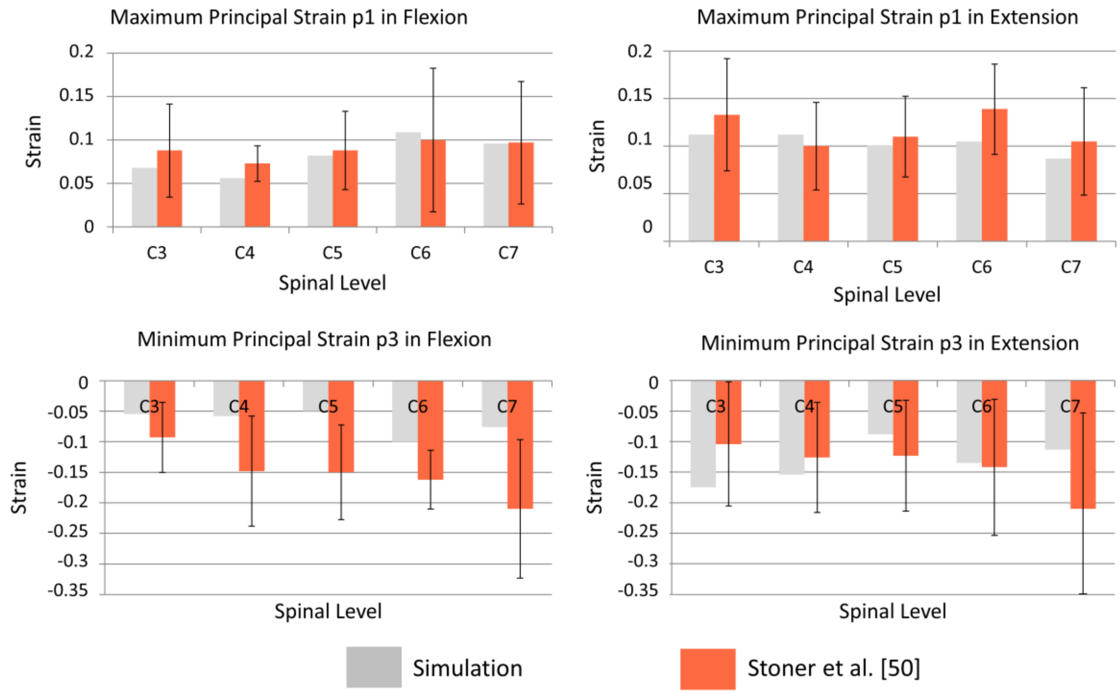

Figure 3: Maximum and minimum principal strains. Error bars represent one standard deviation

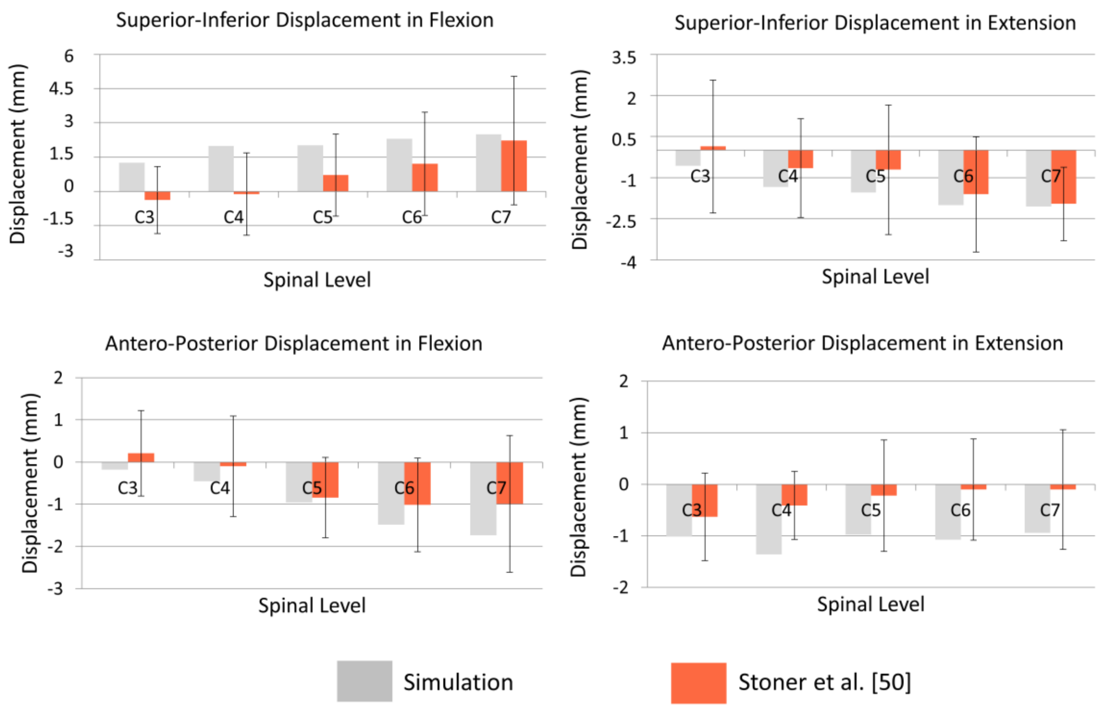

Figure 4: Relative antero-posterior displacements and superior-inferior displacements. Error bars represent one standard deviation

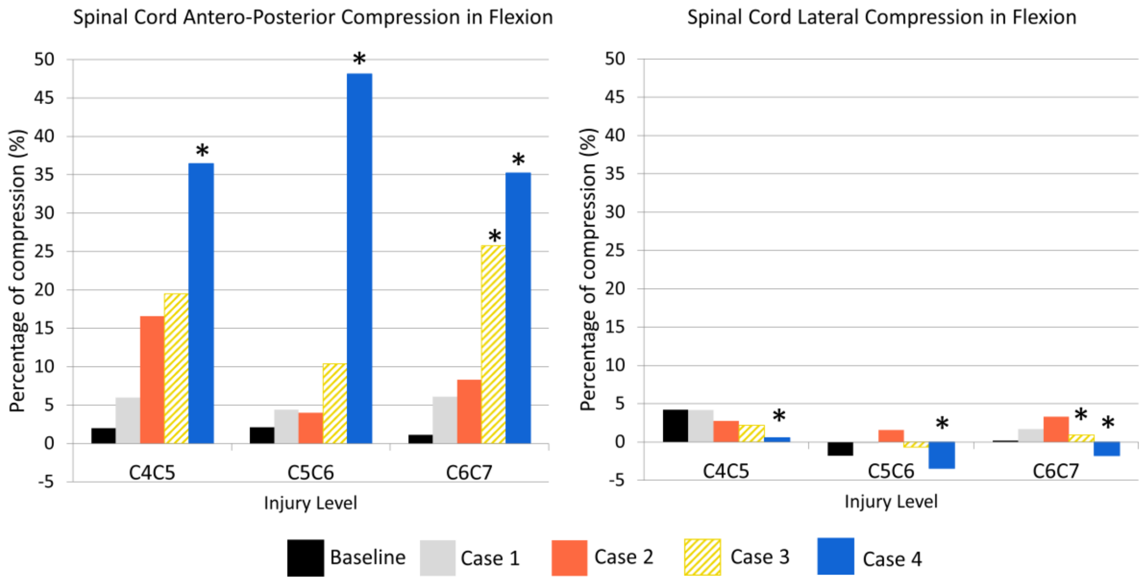

Figure 5: Percentage of spinal cord compression at the injured functional spinal unit at 2 Nm flexion. Asterisk (*) represents the C2-T1 73 degrees threshold

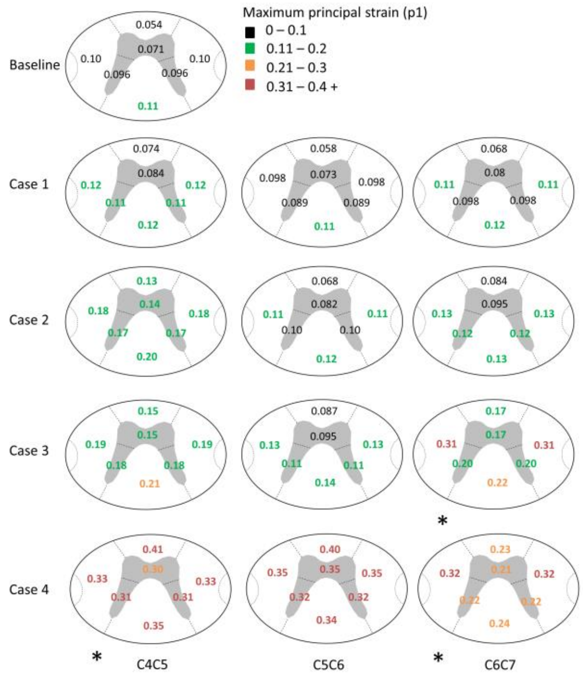

Figure 6: Maximum principal strains p1 in spinal cord by sections at 2 Nm flexion. Asterisk (*) represents the C2-T1 73 degrees threshold

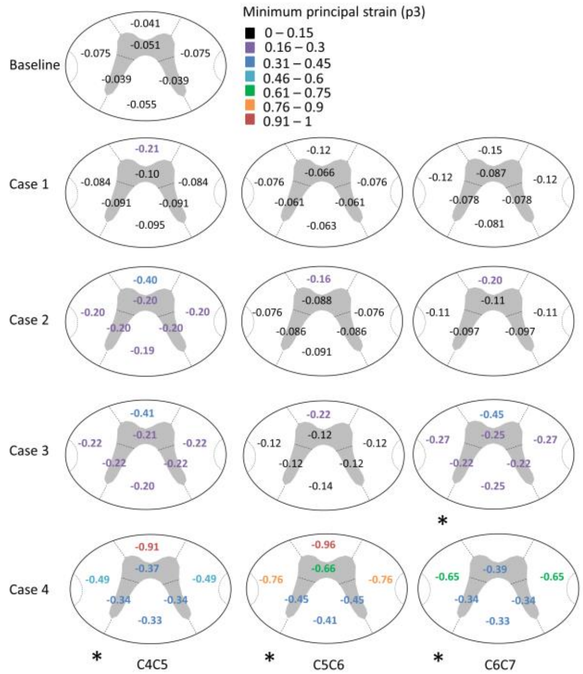

Figure 7: Minimum principal strains p3 in spinal cord by sections at 2 Nm flexion. Asterisk (*) represents the C2-T1 73 degrees threshold

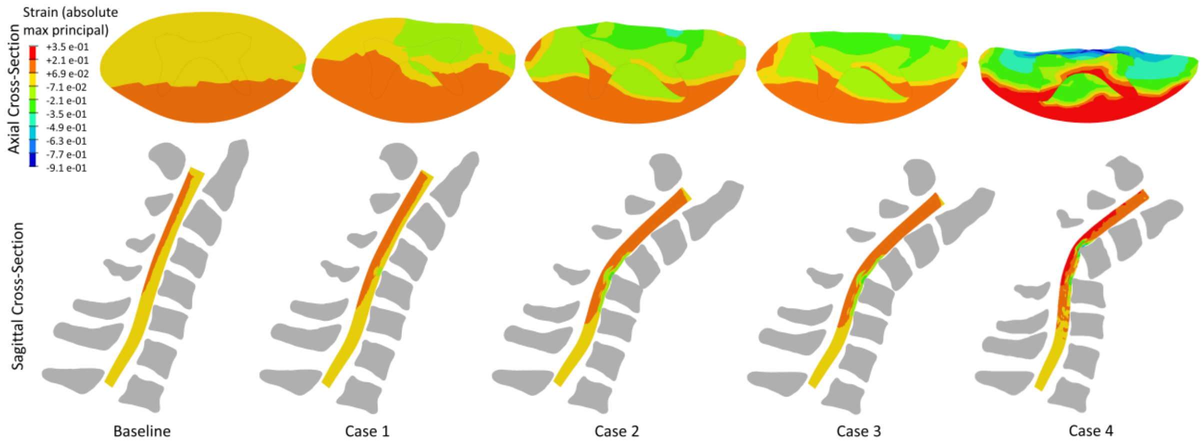

Figure 8: Absolute maximal strain pattern for baseline model and injury models at level C4-C5

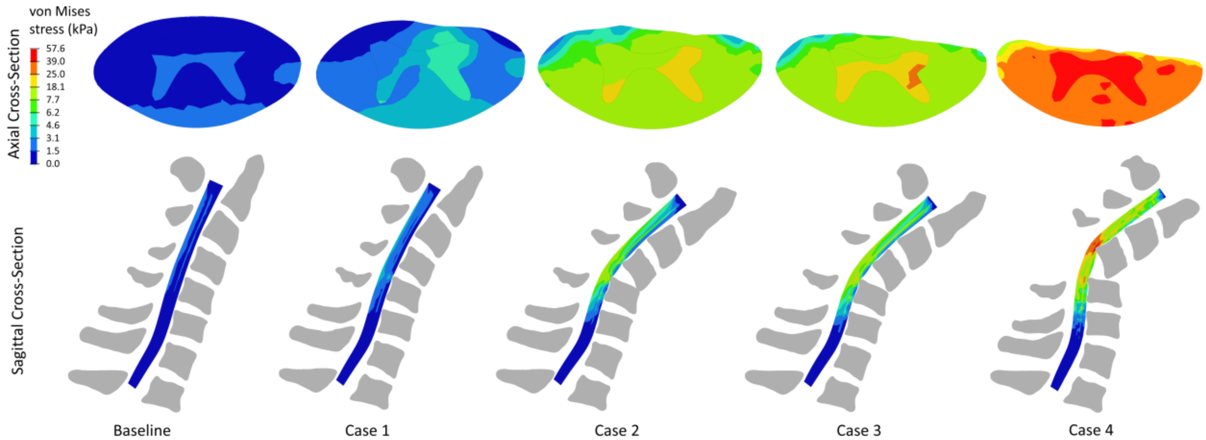

Figure 9: von Mises stress pattern for baseline model and injury models at level C4-C5